Acta Protozool. (2009) 48: 153–170

ACTA
PROTOZOOLOGICA

A New Marine Species of *Amphidinium* (Dinophyceae) from Thermaikos Gulf, Greece

Nicolas P. DOLAPSAKIS and Athena ECONOMOU-AMILLI

Faculty of Biology, Department of Ecology and Systematics, University of Athens, Athens, Greece

Summary. Genus *Amphidinium* Claparède *et* Lachmann (Gymnodiniales, Dinophyceae) *sensu lato* has recently undergone a reappraisal using extended microscopical methods and genetic comparisons, with the type species and morphologically similar species used for the redescription of the genus *Amphidinium sensu stricto*. Within the latter concept of the genus, the new species *Amphidinium thermaeum* is established using light and scanning electron microscopy in combination with LSU rDNA phylogeny. This species was isolated from the Thermaikos Gulf in Greece, and its description is largely based on observations of cultured material. The main diacritic features distinguishing *A. thermaeum* from related taxa were: shape, size and plasticity of the cell, position of distal and proximal cingulum ends, site of longitudinal flagellar insertion, sulcal course, pusule details, plastid characteristics, and mode of cell division. Genetic phylogeny applying Bayesian Inference, Maximum Likelihood, and Neighbor-Joining analyses, places *A. thermaeum* in an independent position within the *Amphidinium sensu stricto* monophyletic group, and the new species is closely related to its small and morphologically similar siblings (*A. massartii*, *A. klebsii*, *A. trulla*, *A. gibbosum*, *A. carterae*).

Key words: *Amphidinium thermaeum* sp. nov., Dinophyceae, microscopy, LSU rDNA, molecular phylogeny.

INTRODUCTION

Species belonging to genus *Amphidinium* Claparède *et* Lachmann, 1859 emend. Flo Jorgensen, Murray *et* Daugbjerg, 2004 are largely autotrophic and cosmopolitan, forming an important part of the benthic dinoflagellate community in sandy saline biotopes (Larsen and Patterson 1990, Steidinger and Tangen 1997, Murray and Patterson 2002, Flø Jørgensen *et al*. 2004a). *Amphidinium* taxa are often observed to participate in algal blooms (e.g., Herdman 1911, Baig *et al*. 2006) and some are toxic to other organisms (cytotoxic, ichthyotoxic, or haemolytic, e.g., Steidinger 1983, Yasumoto *et al*. 1987, Maranda and Shimizu 1996, Murray *et al*. 2004, Baig *et al*. 2006).

Genus *Amphidinium* belongs to the 'naked' dinoflagellates with amphiesma not containing thecal plates, i.e., to Gymnodiniales, Dinophyceae (Fensome *et al*. 1993). Representatives of the old circumscription of the genus exhibit considerable morphological variability, forming a group of species (*Amphidinium sensu lato*) with well over 100 reported taxa (e.g., Schiller 1933, Conrad and Kufferath 1954, Flø Jørgensen *et al*. 2004a, Calado and Moestrup 2005). Certain *Amphidinium* spe-

Address for correspondence: Nicolas P. Dolapsakis, Ecology and Systematics, Department of Biology, University of Athens, Zografou, Athens 15784, Greece; Fax: +30-210-7274885; ndol@biol.uoa.gr

cies present ambiguous taxonomy, some belonging to another genus and others having been poorly or falsely described (Flø Jørgensen *et al*. 2004a, b; Murray *et al*. 2004; Sparmann *et al*. 2008).

Taxa belonging to *Amphidinium sensu lato* are generally characterized by an oval cell shape with an anterior small epicone, and by a cingulum (with none or slight displacement) ventrally tapering to the sulcus (Kofoid and Swezy 1921, Popovský and Pfiester 1990). The traditional diacretic feature of the genus, i.e., 'height of the epicone not exceeding one-third the height of the hypocone' (Steidinger and Tangen 1997) has been found to be taxonomically insufficient (Daugbjerg *et al*. 2000); hence the redescription of the type species *Amphidinium operculatum* and the definition of the genus *Amphidinium sensu stricto* (Flø Jørgensen *et al*. 2004a, Murray *et al*. 2004). While species belonging to *Amphidinium sensu stricto* are accepted as 'true' *Amphidinium* species, their taxonomy is complicated by morphological interspecific similarities and intraspecific cell variability, compounded by plasticity of cells due to gymnodinoid characteristics (Schiller 1933, Daugbjerg *et al*. 2000, Murray *et al*. 2004). Ultimately, it is necessary to identify representatives of *Amphidinium sensu stricto* based not only on careful microscopical examination of cell morphology and plastid (chloroplast) characteristics from cultured material, but also on genetic phylogeny. The most widely assessed gene for *Amphidinium* species has been the large subunit ribosomal RNA gene (Daugbjerg *et al*. 2000, Flø Jørgensen *et al*. 2004a, Murray *et al*. 2004).

Herein, a new species belonging to the genus *Amphidinium sensu stricto* is established using clonal cultures, microscopy and genetic phylogeny. This taxon was isolated from Thermaikos Gulf in Greece, an area known for its extensive harmful algal blooms of various species throughout the year (Nikolaides and Moustaka-Gouni 1990, Moncheva *et al*. 2001, Koukaras and Nikolaidis 2004).

MATERIALS AND METHODS

Sampling and microscopy

Sampling was carried out near the Loudias-Axios rivers' delta system in the area of Malgara, Thessaloniki (Thermaikos Gulf, north-west Aegean Sea) in June 2002. Samples were collected offshore at midday from the water column near the marine sandy bottom (~2m depth), using a one-liter Ruttner plankton sampler from a boat. Salinity at the location was 32 ppt. Sequential isolations by micropipette after enrichment and cultivation of natural samples resulted in two *Amphidinium* clonal cultures, UoABM-Atherm1 and UoABM-Atherm2. Differential interference contrast (Nomarski) microscopy was carried out on live cultured cells using an Axio Imager AX10 microscope system and digitally photographed with an AxioCam MRc camera and Axiovision software (Zeiss, Germany). Epifluorescence microscopy was carried out on live cultured cells using an Axioplan (Zeiss, Germany) equipped with a G365/LP420 (blue), BP 450-490/BP515-565 (green) and BP510-560/LP590+LP (red) filter set and digitally photographed using an Axiocam MRc5 and Axiovision software. For SEM, 5 ml of culture (mid-exponential phase) were fixed with 2% OsO_4 (final concentration buffered with phosphate buffer solution) and prepared according to the method of Botes *et al*. (2002) on round glass cover-slips. The dried sample was gold-plated (Jeol Fine Coat Ion Sputter, JFC-1100) and observed in a Jeol scanning electron microscope, JSM-35 (Japan).

DNA extraction, PCR amplification and sequencing

Approximately 10×10^6 cells in exponential phase of each strain were centrifuged and pelleted in 15 ml tubes and washed several times with 0.2 µm filtered, sterilized seawater. DNA was extracted using a DNeasy Plant Mini Kit (Qiagen, Valencia, CA) following manufacturer's instructions. Primers used for PCR amplification (Saiki *et al*. 1988) of gene sequences were supplied by the Foundation for Research and Technology (Crete, Greece). Primers D1R--forward and D2C-reverse were targeted towards conserved core sequence positions 24-43 and 733-714, respectively, relative to the *Prorocentrum micans* LSU rDNA, amplifying approximately a 700 bp portion that includes the variable domains D1/D2 of the LSU (Lenaers *et al*. 1989, Scholin *et al*. 1994). PCR was carried out using an Invitrogen AccuPrime kit (Carlsbad, CA) following manufacturer's instructions. A TPersonal Combi (Biometra, Germany) was used for 50 µl PCR reactions with thin-walled 0.2 ml Eppendorf tubes and 100 pmol of each primer. PCR cycles were: denaturation at 94°C for 2 min., 35 cycles of 94°C for 1 min., then 52°C for 2.5 min., and 72°C for 2 min. Final extension was at 72°C for 10 min. Successful amplification was confirmed by 1.6% agarose gel electrophoresis and a DNA 50bp-2kb ladder (Sigma-Aldrich). Amplified fragments were gel purified using a Qiagen MinElute Gel Extraction Kit according to manufacturer's instructions. Dye terminator cycle sequencing was carried out by Macrogen (Korea).

Phylogenetic tree construction

Partial LSU sequences obtained for the two isolated *Amphidinium* clones were initially evaluated using the Basic Length Alignment Searching Tool (Altschul *et al*. 1990, Zhang *et al*. 2000) and compared against other deposited sequences in GenBank. The sequences of 32 *Amphidinium* strains (Table 1) along with sequences of the gymnodinoid dinoflagellate *Akashiwo sanguinea* (outgroup) were aligned using ClustalX (Thomson *et al*. 1997). The LSU sequences AJ417899 and AJ417900 belonging to *Amphidinium eilatiensis* were also aligned with the sequences listed in Table 1, but not used in the phylogenetic tree construction process. A total of 781 characters resulted from the sequence alignment, and ambiguous regions were not removed since the use of non-ambiguous alignments gave the same phylogenetic results. Modeltest version 3.7 (Posada and Crandall 1998) was used to estimate the optimal criteria model

Table 1. Taxa used in the phylogenetic analysis along with their strain and accession numbers as deposited in GenBank.

Taxon (strain)	GenBank #
Amphidinium carterae Hulburt, 1957 (CAWD22)	AY460581
Amphidinium carterae Hulburt, 1957 (CAWD23)	AY460582
Amphidinium carterae Hulburt, 1957 (CAWD57)	AY460583
Amphidinium carterae Hulburt, 1957 (CCMP121)	AY460585
Amphidinium carterae Hulburt, 1957 (CCMP124)	AY460584
Amphidinium carterae Hulburt, 1957 (CCMP1748)	AY460586
Amphidinium carterae Hulburt, 1957 (CS-740)	AY460578
Amphidinium carterae Hulburt, 1957 (JL3)	AF260380
Amphidinium carterae Hulburt, 1957 (MFJ1, K-0654)	AY455669
Amphidinium carterae Hulburt, 1957 (SM10)	AY460579
Amphidinium carterae Hulburt, 1957 (SM11)	AY460580
Amphidinium gibbosum (Maranda *et* Shimizu) Flø Jørgensen *et* Murray, 2004 (CCMP 120)	AY455672
Amphidinium gibbosum (Maranda *et* Shimizu) Flø Jørgensen *et* Murray, 2004 (SI-36-50)	AY460587
Amphidinium herdmanii Kofoid *et* Swezy, 1921 (MFJ10, K-0655)	AY455675
Amphidinium herdmanii Kofoid *et* Swezy, 1921 (MFJ5)	AY460595
Amphidinium incoloratum Campbell, 1973	AY455677
Amphidinium klebsii Kofoid *et* Swezy, 1921 (JL9)	AF260381
Amphidinium massartii Biecheler, 1952 (AKLSPO1)	AY460588
Amphidinium massartii Biecheler, 1952 (AKLV01)	AY460589
Amphidinium massartii Biecheler, 1952 (CCMP 1821)	AY455670
Amphidinium mootonorum Murray *et* Patterson, 2002 (MFJ18, K-0656)	AY455676
Amphidinium operculatum Claparède *et* Lachmann, 1859 (CAWD42)	AY460590
Amphidinium operculatum Claparède *et* Lachmann, 1859 (CAWD55)	AY460591
Amphidinium operculatum Claparède *et* Lachmann, 1859 (CAWD56)	AY460592
Amphidinium operculatum Claparède *et* Lachmann, 1859 (SM06)	AY455674
Amphidinium semilunatum Herdman, 1924	AY455678
Amphidinium steinii Lemmermann, 1910 (SM12)	AY460593
Amphidinium steinii Lemmermann, 1910 (SM17)	AY455673
Amphidinium thermaeum Dolapsakis *et* Economou, 2009 (UoABM-Atherm1)	GQ200834
Amphidinium thermaeum Dolapsakis *et* Economou, 2009 (UoABM-Atherm2)	GQ200835
Amphidinium trulla Murray, Rhodes *et* Flø Jørgensen, 2004 (CAWD68)	AY460594
Amphidinium trulla Murray, Rhodes *et* Flø Jørgensen, 2004 (MFJ2, K-0657)	AY455671
Akashiwo sanguinea (Hirasaka) G.Hansen *et* Moestrup, 2000	AF260397
Akashiwo sanguinea (Hirasaka) G.Hansen *et* Moestrup, 2000	AF260396

for phylogeny. Phylogenetic trees of aligned LSU sequences were obtained by Bayesian Inference (BI) using the MrBayes software package 3.1 (Huelsenbeck and Ronquist 2001) with the GTR+G model and 3,000,000 generations at a sample frequency of 10, by Maximum Likelihood (ML) and by Neighbor-Joining (NJ) with the Kimura 2-parameter model (Kimura 1980) using the software RAxML 7.0.4 (Stamatakis 2006, Stamatakis *et al*. 2008) and MEGA 4 (Tamura *et al*. 2007), respectively, with 1000 bootstrap resamplings (Felsenstein 1985). A Maximum Parsimony (MP) tree topology was also produced for comparison using PAUP 4.10 (Swofford 2000). Trees were viewed with the Treeview software (Page 1996).

RESULTS

Amphidinium thermaeum sp. nov., Dolapsakis *et* Economou-Amilli (Figs 1–47)

Descriptio: Cellulae dinoflagellatae, photosyntheticae, solitariae, forma plerumque ovatae, dorsiventraliter compressae, 10–30 µm longae et 8–20 µm latae. Forma saepe mutabilis et aliquantum metamorpha. Epiconus parvus, forma linguae flexae et ad sinistram deflectae, oriens de hypoconi regione ventrali superiore et tendens ad faciem dorsalem. Hypoconus asymmetrus, regione anteriore truncatus et obliquus, antapice rotundus, lateribus convexus. Extremum proximali cinguli situm, longitudine cellulae, 0.15–0.25 ab apice cellulae et extremum distali cinguli situm 0.25–0.40 ab apice cellulae, ambo extrema ventralia. Sulcu incipiens ad centrum faciei ventralis in fissura depressa 2–4 µm ubi origo flagellis longintudinalis. Sulcus primo flexus ad dextram et continuo minime inclinatus ad sinistram, postice pallor et diffusis, plerumque non tangens antipodem cellulae. Pusulae duae, circa 1 µm diametro et circumdatae parvis vesiculis radiaribus, una sub locum proximum principio flagelli transversalis et una ad dextram loci originis flagelli longintudinalis. Mons angustus ventralis loca insertionis flagellatae iungat. Nucleus plerumque rotundus aut ovatus, 4.5–7.5 µm diametro, in parte postica hypoconus. Pyrenoides circularis, in forma annuli et amylo vaginata, 3.5–5.5 µm diametro, centro cellulae. Fulvus chloroplastus, singularis et stellatus, cum lobis numerosis qui ab pyrenoides radiarient ad peripheralem regionem cellulae. Divisio agamica intra cistas hyalinas.

Description: Cells dinoflagellate, photosynthetic, single, typically oval and dorso-ventrally compressed, 10–30 µm long and 8–20 µm wide (average 20 µm long, SD = 3.2 µm and 15 µm wide, SD = 2.1 µm; n = 184 cells). Cell shape often metabolic and partly metamorphic. Epicone small with a bent tongue-like shape and left deflection, arising from the ventral side of the hypocone apex and extending dorsally. Hypocone asymmetric with a truncated and oblique anterior, rounded antapex and convex sides. Proximal and distal ends of cingulum on the ventral side, located at a distance 0.15–0.25 and 0.25–0.40 of the cell length from the apex, respectively. Sulcus beginning near the cell's ventral center in a cleft 2–4 µm deep where the longitudinal flagellum also originates. Sulcus course initially bearing a right bend and continuing with a slight left inclination, becoming shallow, wide and fading posteriorly, usually not reaching the antapex. Two small pusules present, each ca. 1 µm in diameter and surrounded by small radiating vesicles, one immediately below the origin of the transverse flagellum and the other immediately to the right of the origin of the longitudinal flagellum. The two points of flagellar insertion connected by a narrow ventral ridge. Nucleus usually round or oval, 4.5–7.5 µm in diameter, located at the hypocone posterior. Pyrenoid round, ring-like and starch-sheathed, 3.5–5.5 µm in diameter, located at the cell centre. Chloroplast golden-brown, appearing as single and stellate, with numerous lobes radiating from the pyrenoid to the cell periphery. Asexual division within hyaline cysts.

Etymology: from the name of the area where the species was isolated (Thermaikos Gulf, in Latin '*Thermaeus' sinus*).

Holotype: Fig 1.

Type locality: Thermaikos Gulf, Greece.

Habitat: Marine and brackish, sandy benthic habitats.

Supplemental cell characteristics of *Amphiniun thermaeum* are as follows: The widest part of the cell usually appears near the middle and less often towards the cell's anterior or posterior (Figs 2–11, 30–33). The right side of the epicone is inclined to the left and the epicone sides may have a slight or more pronounced bend (Figs 2–5, 39–42). The epicone often exhibits minimal apical rise and the dorsal extension may tightly cover the hypocone's anterior (Figs 40, 44). The hypocone's right side tends to be more convex than the left side. The left anterior side of the hypocone tends to be taller than the right anterior side (Figs 2–5, 39, 40). The hypocone's dorsal side may occasionally exhibit a shallow longitudinal cleavage (Fig. 45). The cingulum is displaced and descending on both ventral and dorsal sides. The distal end of the cingulum tapers to a shallow ventral trench, and the proximal end borders the narrow ventral ridge

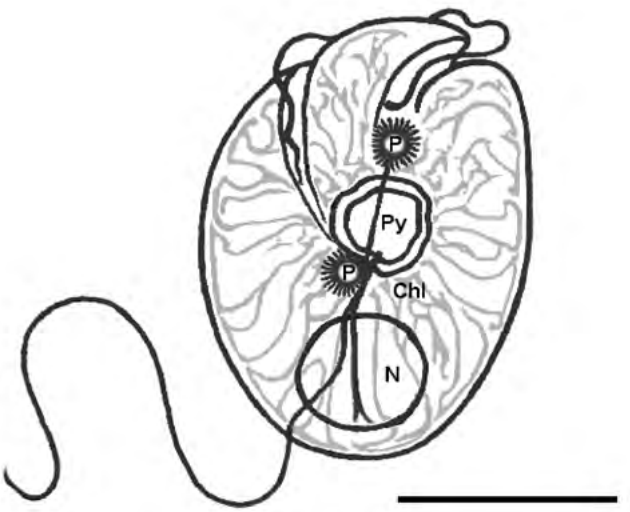

Fig. 1. Line drawing of *Amphidinium thermaeum* (holotype). N – nucleus, Py – pyrenoid, P – pusule, Chl – chloroplast (strands and lobes). Scale bar: 10 μm.

which appears to be grooved; trench and ridge meet at the sulcus's anterior at a 'V' shape, thus contouring ventrally the posterior part of the epicone (Figs 22, 23, 39, 40, 44, 47). Underneath the ventral ridge a canal-like structure appears to join the two pusules, partially incising the pyrenoid (Figs 6, 8). The vesicles that radiate from the two pusules are elongate, resulting in a pusular system often > 3 μm in diameter (Figs 6, 7). The sulcal cleft is partially hidden by an arched cover resulting in a characteristic right bend in the sulcal course (Figs 22, 23). The plastid appears to extend fully in the hypocone and partially into the epicone as well, and the chloroplast lobes may appear as stringy, slim or dilated, with ramifications or a slight reticulation (Figs 12–17). A group of 4–5 adjacent vacuolar bodies can be seen to the left of the longitudinal flagellar insertion, appearing as circular depressions within the hypocone (Figs 26––27). The cell surface may be smooth with small sparse nodules (Fig. 39) and a shallow amphiesmal vesicle pattern (Figs 42, 43), or it may be observed as 'pubescent' due to remnants adhering to cell surface after cyst lysis (Fig. 40). Storage bodies, assimilation granules and smaller red bodies are observed throughout the cell (Figs 9–11). There is mucus production by the cells.

Close observation of cultured material showed morphological variations from the above typical description. Oblong or sac-like cell forms are common in late or post-exponential culture phase, whereas more spherical forms are common during the early exponential culture phase (sometimes with reduced swimming activity) (Figs 30–33). In oblong or sac-like cells, concave sides or a more leveled antapex may be observed. In spherical cells, the convexity of the hypocone sides tends to be the same. The left deflection of the epicone can be minimal or extreme (Figs 45, 46). The sulcus may sometimes reach the antapex, resulting in a lobed cell posterior region (Fig. 24). The pusules are not always visible. The nucleus may also be observed as reniform. In certain cells there are two pyrenoids or one that is deformed or dividing (Figs 24, 25). A spherical mass may sometimes be observed in differing regions of the cell (Figs 28, 29). Rarely, one or two large vacuoles may be observed in the hypocone (Figs 37, 38). Very rarely, distorted cells may appear with striations or furrows on the hypocone (Fig. 36).

Sequence comparison

The partial LSU (D1/D2 region) rDNA sequence of *Amphidinium thermaeum* diverges 13–22% from sequences belonging to the group of species *A. massartii* / *A. klebsii* / *A. trulla* / *A. gibbosum* / *A. carterae*, and 33–46% from sequences belonging to the group of species *A. operculatum* / *A. steinii* / *A. mootonorum* / *A. hermanii* / *A. incoloratum*. The smallest intraspecific divergences between all the examined sequences were found to be ~6–8% (*A. massartii*, *A. carterae* strains). The interspecific variation between the sequence of *A. mootonorum* strain MFJ18 and those of *A. herdmanii* strains MFJ5 and MFJ10 was found to be < 2%. The LSU sequences AJ417899 and AJ417900 belonging to *A. eilatiensis* were found to be identical to the sequences AY460578, AY460579, AY460580, AY460583, AY460584 belonging to various *A. carterae* strains (see Table 1).

Genetic phylogeny

The partial LSU (D1/D2 region) rDNA sequences of the two *A. thermaeum* strains UoABM-Atherm1 and UoABM-Atherm2 were identical. The three phylogenetic trees produced (Figs 48–50) applying Bayesian Inference, Maximum Likelihood and Neighbor-Joining analyses to the available partial LSU sequences of *Amphidinium* species sensu stricto (see Table 1) resulted in the clear placement of *Amphidinium thermaeum* in a closely related, yet independent clade (at 100% probability). Specifically, this species was phylogenetically positioned between the *A. massartii* / *A. klebsii* / *A. trul-*

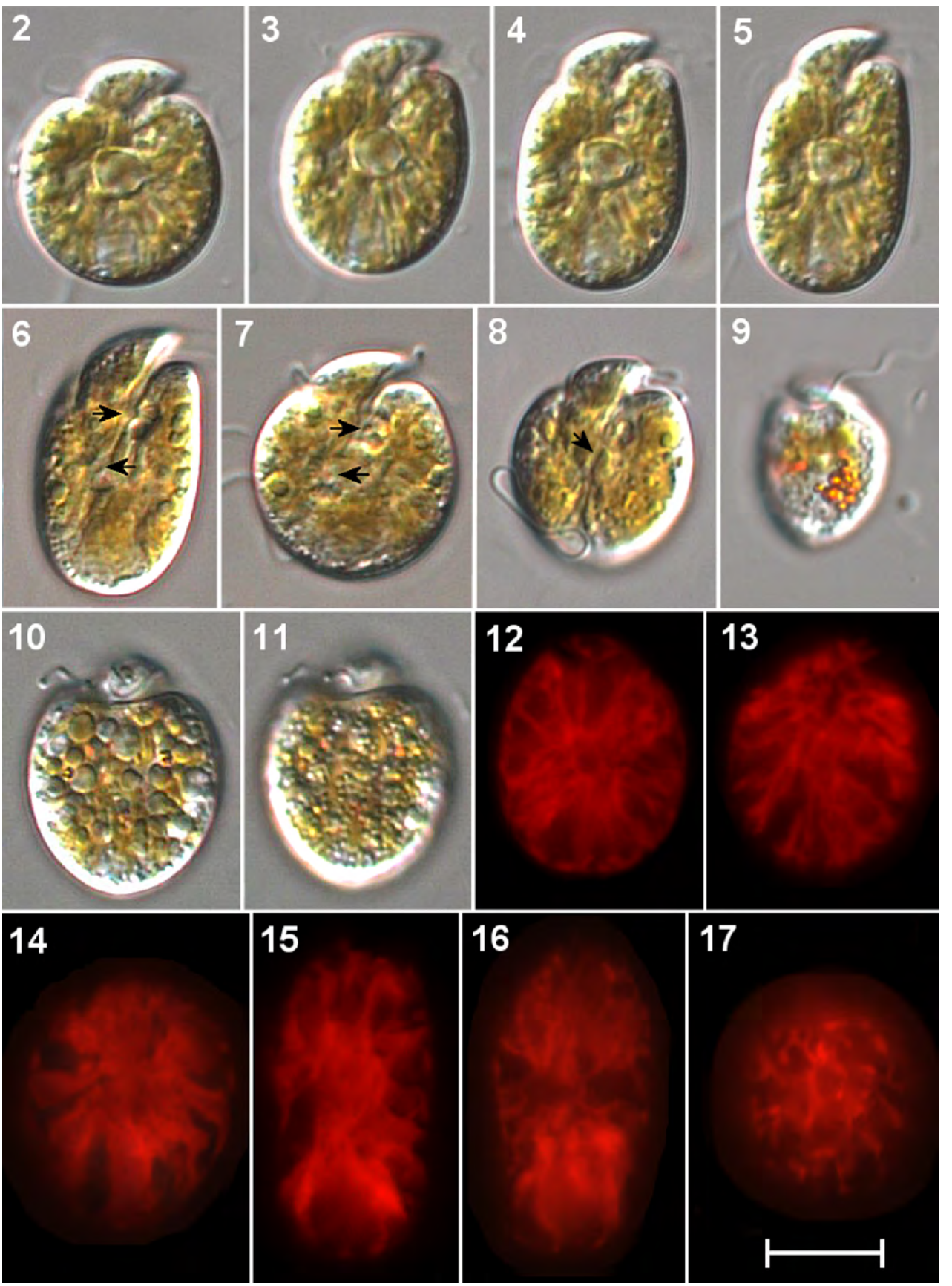

la / *A. gibbosum* / *A. carterae* group of clades and the *A. operculatum* / *A. steinii* / *A. mootonorum* / *A. hermanii* group of clades. The three phylogenetic trees varied a little as to the placement of the *A. operculatum* clade and the *A. trulla* / *A. gibbosum* clade, but the distinct and separate position of *Amphidinium thermaeum* remained unchanged in the three applied analyses. Posterior probabilities in BI were generally very high (≥ 87%), except for the *A. operculatum* clade (76%) and the *A. trulla*/ *A. gibbosum* clade (53%). Certain bootstrap values in the ML and NJ analyses were lower as compared to the BI posterior probabilities, but the general topology was well supported throughout. There was no significant separation between the *A. mootonorum* strain MFJ18 and the *A. herdmanii* strains MFJ5 and MFJ10. The clade containing the strains *A. massartii* CCMP1821 and *A. klebsii* JL9 differentiated significantly from the clade containing the two *A. massartii* strains, AKLV01 and AKLSP01. Sequences belonging to *A. operculatum* strains exhibited the largest genetic distance compared with other *Amphidinium* species. The species *A. incoloratum* appears as the earliest divergent of the monophyletic group *Amphidinium* species *sensu stricto*, while the strain named '*A. semilunatum*' appeared as an independent taxon in all analyses, diverging significantly from the *Amphidinium* group. Maximum Parsimony analysis (not presented here) resulted in an identical topology as that produced by BI, except for a closer relationship of the *A. operculatum* clade to the *A. mootonorum* / *A. herdmanii* / *A. steinii* clades.

DISCUSSION

Morphological similarities between many of the currently known 20 species of *Amphidinium sensu stricto* cause taxonomical confusion (Flø Jørgensen *et al*. 2004a, b; Murray *et al*. 2004), furthermore exacerbated by the fact that different *Amphidinium* species studied in wild samples tend to share similar or misleading (i.e., intraspecifically variable) morphological characteristics (e.g., Larsen 1985, Al-Qassab *et al*. 2002, Murray *et al*. 2004). The current study (and others, e.g., Herdman 1924b, Fukuyo 1981) shows that some of the important taxonomical features cannot be properly ascertained (e.g., cell shape and size, chloroplast structure, pusules) when examining a limited number of cells or when cell 'health' deteriorates (including stressed cells). Therefore, distinguishing *Amphidinium sensu stricto* species can only be done after careful morphological observation of cultured cells during various life stages, combined with DNA analysis.

The establishment of *A. thermaeum* as a new taxon of *Amphidinium sensu stricto* is supported by specific features (i.e., cell shape, size and plasticity, position of distal and proximal cingulum extremes, site of longitudinal flagellar insertion, sulcal course, pusule details, plastid characteristics, and mode of cell division, see Table 2), a combination of which has not been previously reported elsewhere within a specific taxon (see Lemmermann 1910; Kofoid and Swezy 1921; Herd-

Figs 2–17. Photomicrographs of live *Amphidinium thermaeum* cells, (**2**–**11**) under differential interference contrast microscopy and (**12**–**17**) epifluorescence microscopy. **2**–**11** – cells observed in ventral (**2**–**8**), dorsal (**10**–**11**) and lateral view (**9**); **2**–**5** – frame series of one specimen showing 'metabolic movement'; **6**–**7** – the two pusules in an oblong and a subspherical cell, indicated by arrows; **8** – the canal-like structure that joins the two pusules which partially incises the pyrenoid, indicated by an arrow; **9** – small cell with red bodies; **10**–**11** storage bodies and assimilation granules of the same cell under different focal depths; **12**–**16** – the chloroplast with variably structured radiating lobes in ovoid (**12**–**14**) and oblong (**15**–**16**) specimens; **17** – chloroplast lobe terminals near the cell surface. Scale bar: 10 μm.

Figs 18–33. Photomicrographs of live *Amphidinium thermaeum* cells under differential interference contrast microscopy. **18**–**19** – ventral view showing the ventral ridge, indicated by an arrow; **20**–**21** – ventral view showing the central point of longitudinal flagellar insertion, indicated by an arrow; **22**–**23** – ventral view showing the contours of the epicone's posterior forming a 'V' shape on the hypocone and the arched sulcal cleft cover, indicated by an arrow; **24** – dorsal view showing dividing pyrenoid, truncated and oblique hypocone anterior and lobed posterior; **25** – dorsal view showing two pyrenoids, indicated by a pair of arrows; **26**–**27** – ventral view showing a group of 4–5 adjacent vacuolar bodies to the left of the longitudinal flagellar insertion appearing as circular depressions within the hypocone, indicated by an arrow; **28**–**29** – dorsal view showing a spherical mass in different parts of the hypocone, indicated by an arrow; **30**–**33** – different cell shapes (saccular, oval, spherical and oblong respectively) attributed to cell plasticity with the widest region located at the posterior (30), anterior (31, 33) and middle (32) part of the cell.

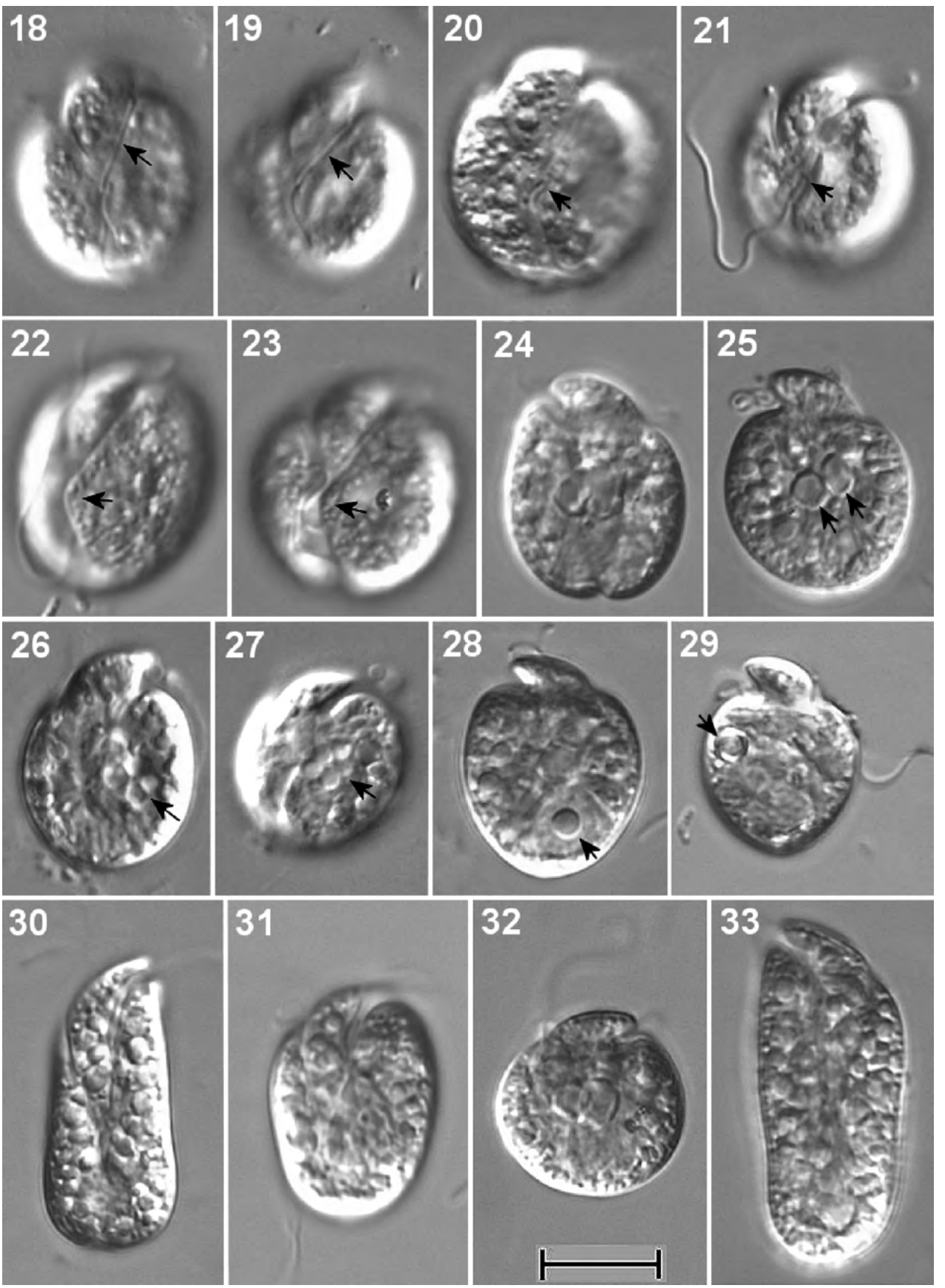

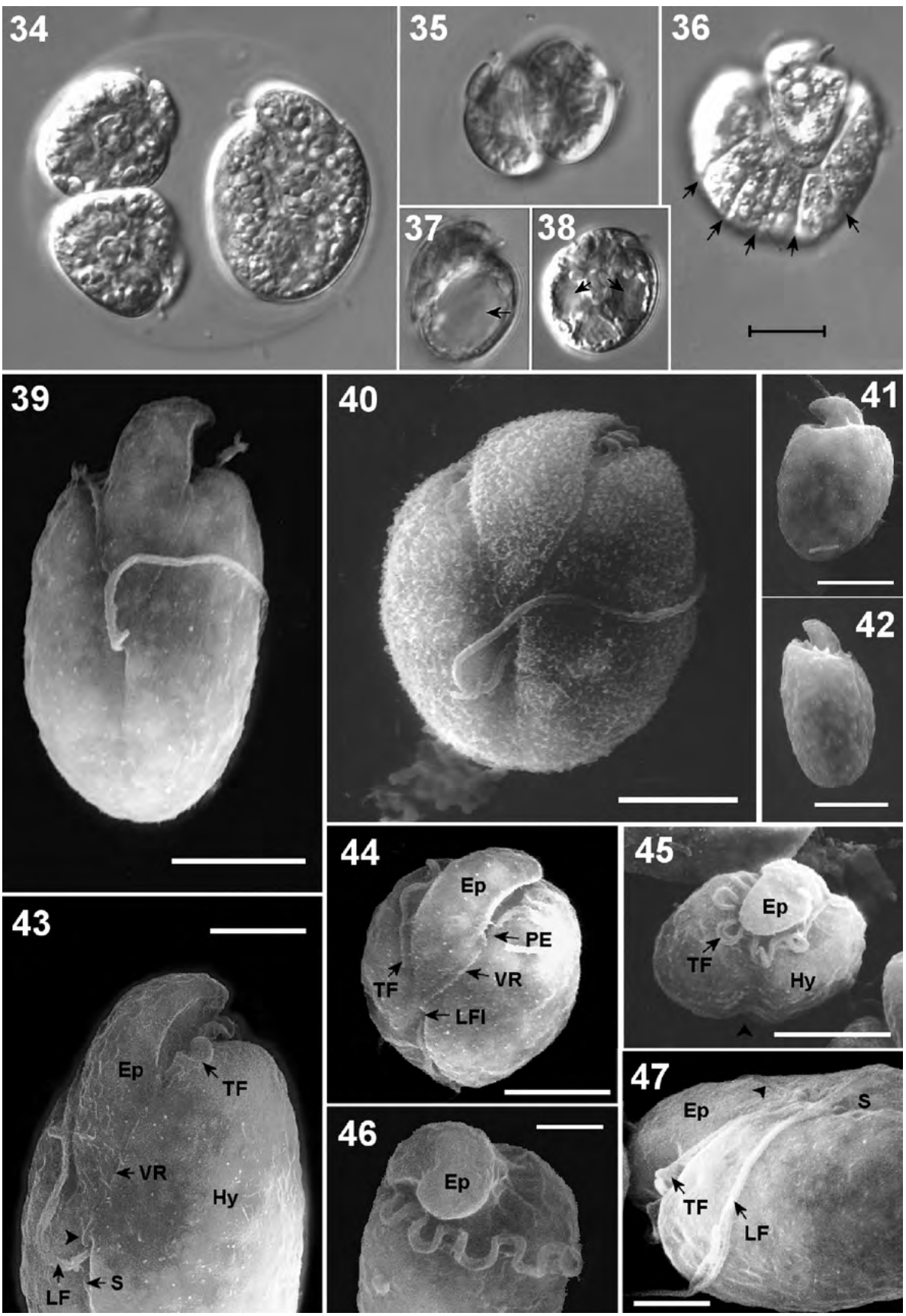

man, 1911, 1922, 1924a, b; Lebour 1925; Schiller 1933; Biecheler 1952; Conrad and Kufferath 1954; Schiller and Diskus 1955; Grell and Wohlfarth-Bottermann 1957; Hulburt 1957; Dodge and Crawford 1968; Taylor 1971; Campbell 1973, Fukuyo 1981; Larsen 1985; Barlow and Triemer 1988; Farmer and Roberts 1989; Klut *et al*. 1989; Larsen and Patterson 1990; Popovský and Pfiester 1990; Maranda and Shimizu 1996; Al-Qassab *et al*. 2002; Murray and Patterson 2002; Flø Jørgensen *et al*. 2004a; Murray *et al*. 2004; Calado and Moestrup 2005; Mohammad-Noor *et al*. 2006). It was noted herein that the general description (Lee *et al*. 2003) and genotype (sequences AJ417899 and AJ417900) belonging to the species *A*. *eilatiensis* likely represent the species *A*. *carterae* and were therefore not considered in our analyses.

There are morphological similarities between *A*. *thermaeum* and the species *A*. *klebsii*, *A*. *steinii*, *A*. *wislouchi* and *A*. *höfleri* (including size overlap, see Table 2), which cannot exclude the possibility of confusion in species identification and a potentially wider geographic distribution of *A*. *thermaeum*. The species *A*. *wislouchi* (Hulburt 1957) was stated as being synonymous with *A*. *steinii* by Murray *et al*. (2004). However, morphological comparison shows that *A*. *wislouchi* might be synonymous to specimens reported as *A*. *klebsii* instead, agreeing with the views of Taylor (1971) and Campbell (1973) who furthermore consider *A*. *wislouchi* as having a single lobed plastid rather than the numerous chromatophores reported by Hulburt (probably due to the obscure nature of the lobes without exhaustive observations). The obvious differences between *A*. *thermaeum* and *A*. *steinii* are the latter's larger cell size, a smaller epicone whose base does not extend as much dorsally, the more anterior position of the longitudinal flagellar insertion with the adjacent pusule placed on its left, the apparent lack of a pronounced sulcal cleft cover, and a larger nucleus. The differences between *A*. *thermaeum* and *A*. *klebsii* are not so clear, but still distinct. Even though some specimen descriptions of *A*. *klebsii* (see Table 2) may not be identical to the original description by Kofoid and Swezy (i.e., possibly representing other species) and certain morphological features have been overlooked (or incorrectly reported), this species differentiates from *A*. *thermaeum* due to its larger cell size, smaller epicone, smaller displacement of the cingulum ends, more anterior position of the longitudinal flagellum and sulcal origins, shallow position of the longitudinal flagellar insertion without a pronounced cleft cover, right deflection of the sulcal course, more anterior position of the pyrenoid, and larger nucleus. Since *A*. *klebsii* has not been studied using epifluorescence microscopy, we abstain from comparing the chloroplast lobes. The differences between *A*. *höfleri* (Schiller and Diskus 1955) and *A*. *thermaeum* are listed in Table 2, but the unusual characteristics of the central position of the nucleus and the posterior position of a large vacuole need to be confirmed in the former species.

The applied phylogenetic analyses using partial LSU rDNA sequences place *Amphidinium thermaeum* independently from other taxa, but within the *Amphidinium sensu stricto* group, therefore supporting its establishment as a new species. The use of the D1/D2 LSU rDNA region (ca. 700 bp) was found to be adequate in securely delineating different species of *Amphidinium sensu stricto*. More importantly, homology was observed between the phylogenetic tree topologies (and structural integrities) produced in this study and those reported by

◀◀

Figs 34–47. Photomicrographs of *Amphidinium thermaeum*, live cells (34–38) under differential interference contrast microscopy and fixed cells (39–47) under scanning electron microscopy. **34** – large cyst with 3 daughter cells; **35** – smaller cyst with 2 daughter cells; **36** – apical view of cell showing unusual furrows on the hypocone, indicated by arrows; **37**–**38** – cells showing one or two rare vacuoles in the hypocone, indicated by arrows; **39** – ventral view of oblong cell with smooth amphiesma showing the more convex right side of the hypocone; **40** – ventral view of spherical cell with 'pubescent' amphiesma covering and with a minimal apical rise of the epicone; **41**–**42** – right dorsal views illustrating the truncated and oblique hypocone anterior, the descending nature of the cingulum and the shallow amphiesmal vesicle pattern; **43** – cell's anterior left side illustrating the ventral ridge's lower end protruding slightly into the sulcal region (arrowhead) and the epicone arising from the ventral side of the hypocone apex, having a shallow amphiesmal vesicle pattern; **44** – apicoventral view of a spherical cell illustrating various morphological features and a minimal apical rise of the epicone which extends dorsally, tightly covering the hypocone's anterior; **45** – apical view of a cell showing the dorso-ventral compression, the left deflection of the epicone and the occasional shallow longitudinal cleavage on the hypocone's dorsal side, indicated by an arrowhead; **46** – apicodorsal view of a cell showing a case of extreme left deflection of the epicone; **47** – cell's anterior right side showing the grooved ventral ridge (arrowhead). Ep – epicone, Hy – hypocone, TF – transverse flagellum, LF – longitudinal flagellum, LFI – longitudinal flagellum's point of insertion, PE – proximal end of the cingulum, S – sulcus VR – ventral ridge. Scale bars: 10 μm, except for Figs 43, 46 and 47 (5 μm).

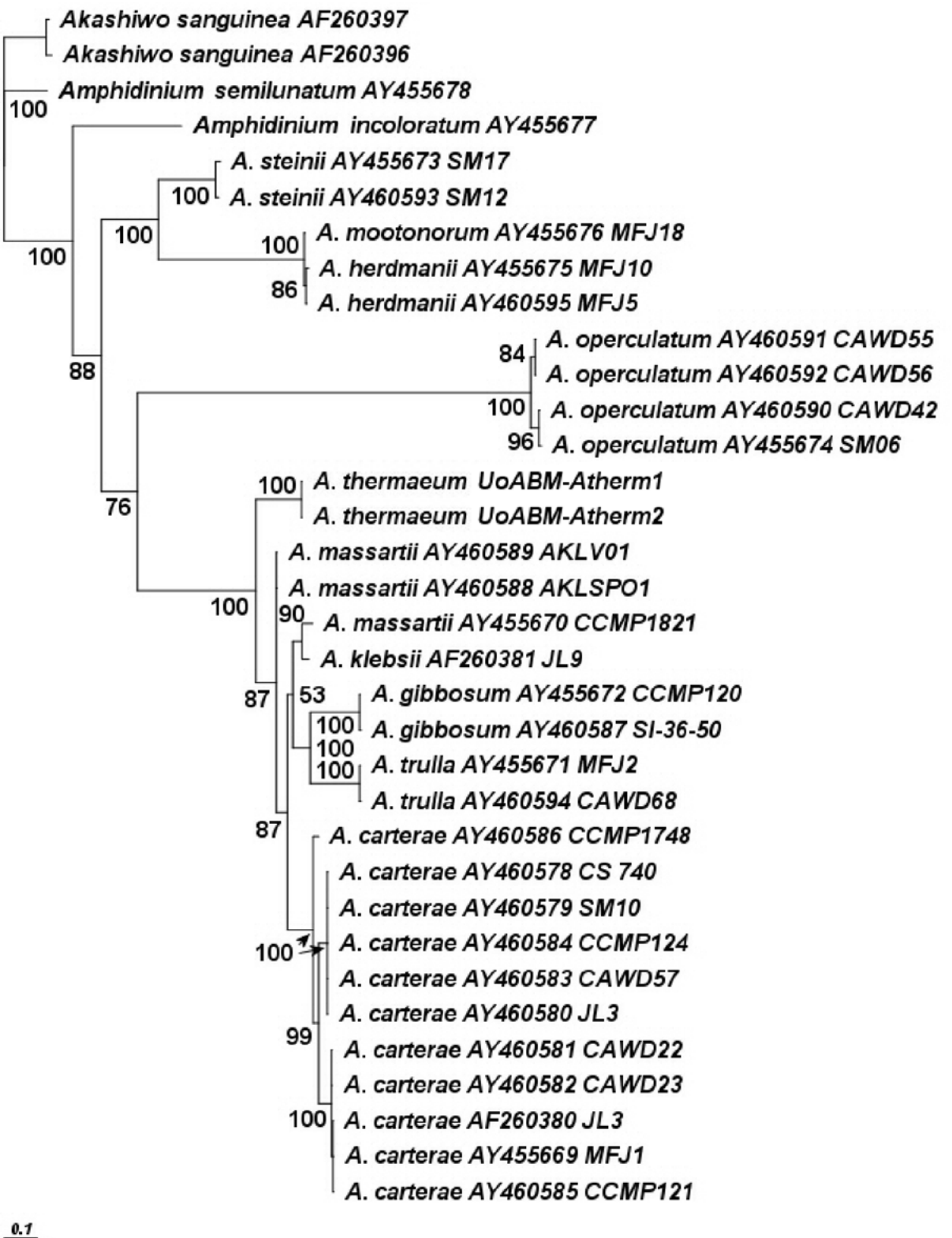

Fig. 48. Bayesian Inference consensus phylogenetic tree obtained from the aligned partial (D1–D2 regions) LSU sequences of two *Amphidinium thermaeum* strains with another 29 strains belonging to *Amphidinium sensu stricto* and 1 strain of *A. semilunatum*, using two strains of *Akashiwo sanguinea* (Gymnodiniales) as an outgroup. Only posterior probabilities > 50% are shown. Scale bar – substitutions/site.

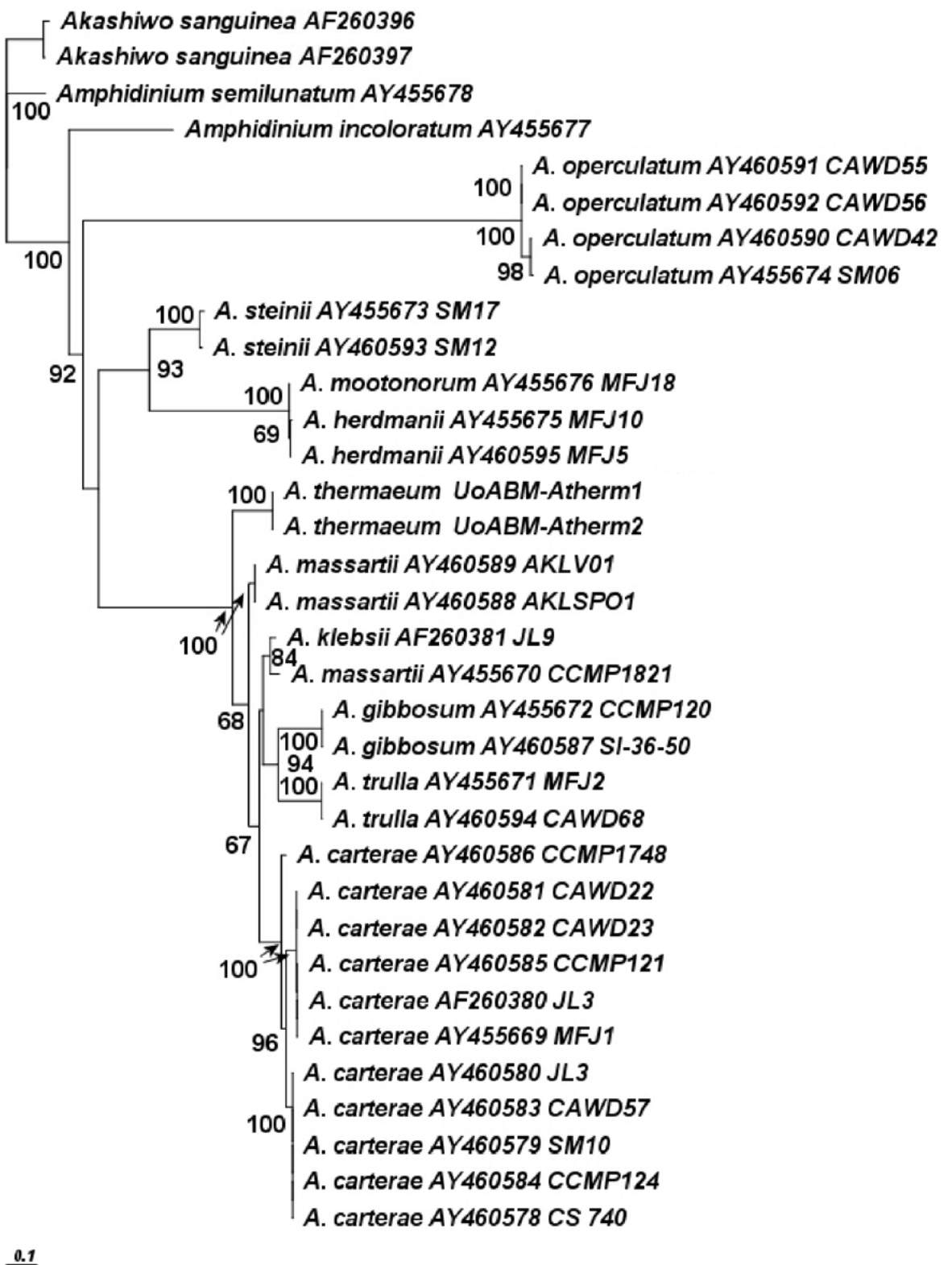

Fig. 49. Maximum Likelihood best-scoring phylogenetic tree obtained from the aligned partial (D1–D2 regions) LSU sequences of two *Amphidinium thermaeum* strains with another 29 strains belonging to *Amphidinium sensu stricto* and 1 strain of *A. semilunatum*, using two strains of *Akashiwo sanguinea* (Gymnodiniales) as an outgroup. Only bootstrap values > 50% are shown. Scale bar – substitutions/site.

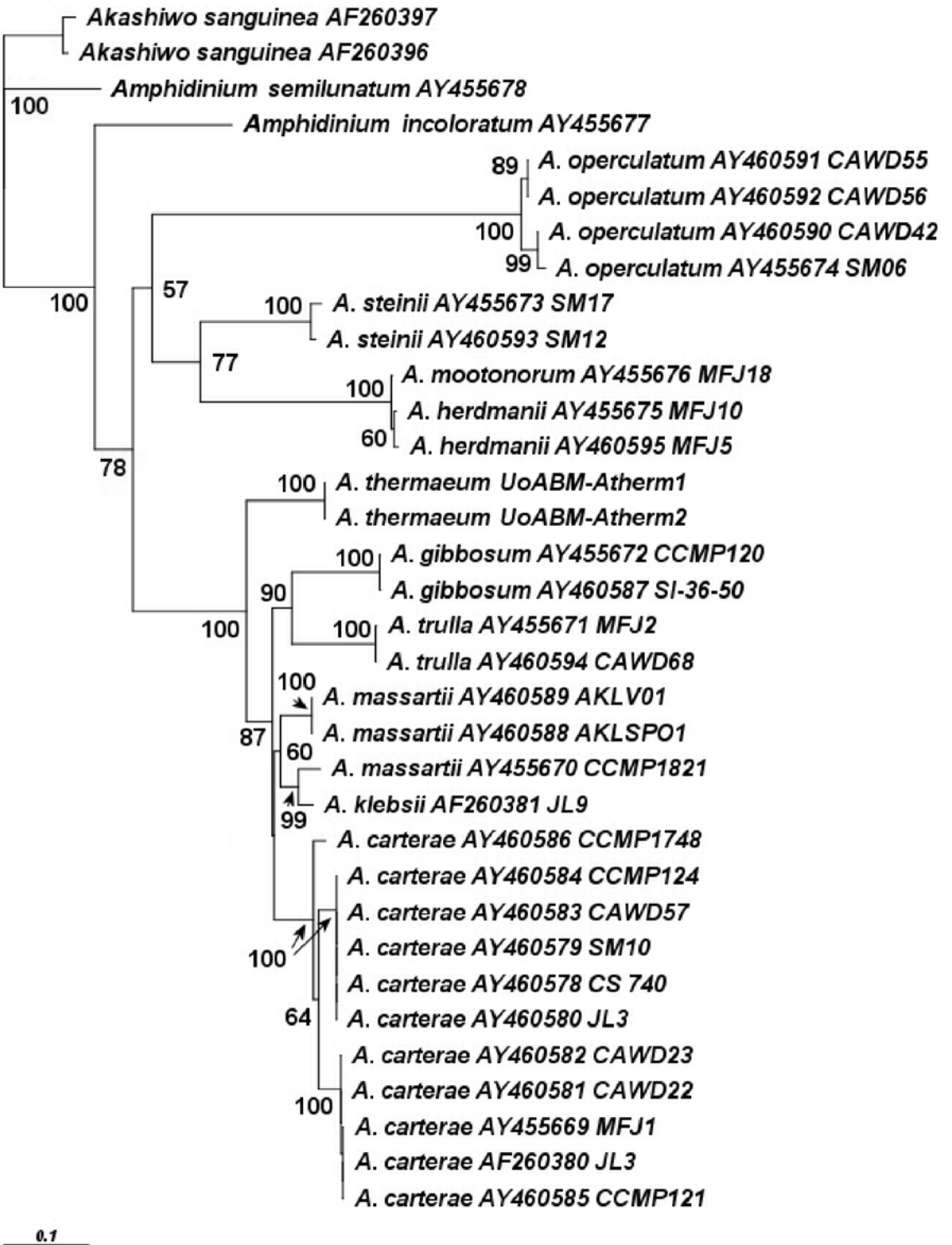

Fig. 50. Neighbor-Joining consensus phylogenetic tree (using the Kimura-2 parameter model) obtained from the aligned partial (D1–D2 regions) LSU sequences of two *Amphidinium thermaeum* strains with another 29 strains belonging to *Amphidinium sensu stricto* and 1 strain of *A. semilunatum*, using two strains of *Akashiwo sanguinea* (Gymnodiniales) as an outgroup. Only bootstrap values > 50% are shown. Scale bar – substitutions/site.

Table 2. Discriminating characteristics of selected *Amphidinium sensu stricto* species.

Species	Size[1]	Shape[2]	CIN[3]	L.F.[4]	PUS[5]	CHL[6]	NUC[7]	PYR[8]	CYS[9]	MET[10]
Amphidinium carterae	10–20 × 6–15 (15 × 10)	Ovoid	P = 0.3–0.4; D = 0.5	Anterior to central	Two, each next to flagellar insertion	Single, with radiating lobes and superficial perforated structure	Posterior; spherical or ovoid, 6–7 µm	Central or slightly anterior, 3 µm	No	No
Amphidinium gibbosum	24–43 × 15–23 (33 × 20)	Cordate to ellipsoid; pointed antapex	P = N/A; D = 0.3	Anterior to central	One (~4 µm) near longitudinal flagellar insertion	Single with thin stellate lobes	Posterior; spherical or ovoid, 10–12 µm	Central, 5 µm	No	Yes
Amphidinium höfleri	19–23 × 13–17	Ovoid to ellipsoid	N/A	Central	N/A	Multiple, independent and spherical	Central; spherical, ~5 µm	Absent	No	No
Amphidinium klebsii	46 × 28[a]; 25–36 × 17–28[b]; 20–40 × 12–24[c]; 16–37 × 11–25[d]	Ovoid, spherical, saccular or elongate [a–d]; hypocone with furrows or striated [a, b]	P or D = 0.2 (?) [a]; P = D [c]; displaced [b,d];	Anterior [a]; anterior to central [b,d]; central [c]	Two (?)[b,d]; N/A[a,c]	Single with stellate lobes[a–d]; reticulated[b] (?)	Posterior; spherical, to ovoid, ~6–15 µm[a–d]; crescentic [b]	Central or slightly anterior, 3–5 µm[b–d]; N/A[a]	Yes[b]; N/A[a,c,d]	Yes[b,d]; N/A[a, c]
Amphidinium massartii	13–22 × 7–17 (17 × 12)	Ovoid	P = 0.3; D = 0.5–0.6	Central	Absent	Single with partially radiating lobes	Posterior; spherical, ovoid or crescentic, 5–6 µm	Left anterior, 2–4 µm	No	No
Amphidinium operculatum	29–50 × 15–36 (37 × 24)	Ovoid to ellipsoid	P = 0.3; D = N/A	Posterior	Two (~2 µm), each next to flagellar insertion	Multiple, independent and elongated	Posterior; ovoid or crescentic, 10–18 µm	Absent (?)	No	No
Amphidinium rhynchocephalum	17–23 × 10–12	Ovoid with conical epicone and ellipsoid to cordate hypocone	N/A	Posterior	Two, each next to flagellar insertion (?)	Single with stellate lobes (?)	N/A	Central or slightly posterior, 4 µm (?)	Yes (?)	Yes (?)
Amphidinium steinii	20–45 × 10–32 (30 × 22)	Ovoid	P = 0.2; D = 0.3–0.4	Anterior	Two (~1 µm), each next to flagellar insertion	Single with stellate strands; reticulate	Posterior; spherical or ovoid, 9–10 µm	Central, 4–5 µm	Yes	Yes
Amphidinium thermaeum	10–30 × 8–20 (20 × 15)	Ovoid, spherical, saccular or oblong	P = 0.15–0.25; D = 0.25–0.40	Central	Two (~1 µm) , each next to flagellar insertion	Single with stellate lobes; ramified	Posterior; spherical, ovoid or crescentic, 4.5–7.5 µm	Central, 3.5–5.5 µm	Yes	Yes
Amphidinium trulla	18–30 × 12–25 (25 × 18)	Ovoid to saccular	P = 0.10–0.15; D = 0.3–0.4	Anterior to central	Absent	Single; stellate lobes	Posterior; spherical, 7–9 µm	Central or slightly anterior, 5 µm	No	No
Amphidinium wislouchi	20–25 × 14–16.5	Ovoid	N/A	Anterior	N/A	Single with stellate lobes	Posterior; spherical, to ovoid	Slightly anterior	N/A	N/A

[1] Cell length × width (µm) with the average indicated in parentheses where available; [2] cell shape; [3] distance of the proximal (P) and distal (D) ends of cingulum from the cell's apex as compared to total cell length; [4] site of longitudinal flagellar insertion (approx. the same with the sulcus origin); [5] pusule size and location; [6] chloroplast characteristics; [7] details of the nucleus; [8] pyrenoid size and location; [9] asexual division within hyaline cysts; [10] cell plasticity and/or 'metabolic movement'. 'N/A' – not available, '?' – needing confirmation. [a] *sensu* Kofoid and Swezy 1921; [b] *sensu* Lebour 1925, Taylor 1971, Fukuyo 1981, Blanco and Chapman 1987, Barlow and Triemer 1988; [c] *sensu* Herdman 1922, 1924a, b; [d] *sensu* Campbell 1973. For other sources see list in discussion.

Murray *et al*. (2004) and Flø Jørgensen *et al*. (2004a), with some insignificant variations. In addition, overall results of the BI, ML, NJ and MP analyses in the current investigation were found to converge.

Amphidinium thermaeum shares general morphological similarities with species closely related in the phylogenetic trees (i.e., *A*. *massartii*, *A*. *klebsii*, *A*. *trulla*, *A*. *gibbosum* and *A*. *carterae*). In contrast, although *A*. *thermaeum* is also morphologically comparable with *A*. *steinii*, these two species exhibit substantial genetic distance. The evident morphological differences of the group of species *A*. *mootonorum* / *A*. *herdmanii* / *A*. *operculatum* / *A*. *incoloratum* (the latter furthermore devoid of chloroplasts; see Campbell 1973) from the group of species *A*. *massartii* / *A*. *klebsii* / *A*. *trulla* / *A*. *gibbosum* / *A*. *carterae* is corroborated by their differentiation in the phylogenetic trees (Figs 48–50). The sequence belonging to '*A*. *semilunatum*' Herdman (accession number AY455678) is separated from the *Amphidinium sensu stricto* group of species because it belongs to *Amphidinium* sensu lato and needs to be redescribed and reclassified.

Cell plasticity (and/or 'metabolic movement') observed in *A*. *thermaeum* has been previously mentioned for various *Amphidinium* species by Massart (1920), Herdman (1924b), Anissimowa (1926), Campbell (1973), Barlow and Triemer (1988), Maranda and Shimizu (1996), and Murray *et al*. (2004). Such observations enhance the view that this trait could be typical for the genus. This type of plasticity is not unusual for gymnodinoid dinoflagellates (e.g., Gaines and Elbrächter 1987, Gómez 2007) and could also be associated with the proposition that *Amphidinium* is an early divergent in the dinoflagellate lineage (Daugbjerg *et al*. 2000, Zhang *et al*. 2007), possibly indicating a constant relation to other protist lineages that exhibit notable cell plasticity (e.g., Larsen and Patterson 1990, Al-Qassab *et al*. 2002). The faint gymnodinoid amphiesmal pattern seen on *A*. *thermaeum* cells is similar to that observed for other *Amphidinium* species, but not as distinct and polygonal as that of *A*. *carterae* (see Klut *et al*. 1989, Murray *et al*. 2004). It is noted that fixing *A*. *thermaeum* cells for optical microscopy often resulted in deformations of amphiesma and chloroplasts, suggesting that cell morphology investigations should be carried out preferably on live cells.

The ventral ridge connecting the two points of flagellar insertion is noted not only in various *Amhidinium* species *sensu stricto* (e.g., Dodge and Crawford 1968, Klut *et al*. 1989, Murray *et al*. 2004), but also in other gymnodinoid representatives from genera such as *Gyrodinium* (Hansen and Daugbjerg 2004) and *Karlodinium* (Bergholtz *et al*. 2005). In the latter two, a relation between the flagellar apparatus and structures underlying the ventral ridge is reported (see also Farmer and Roberts 1989). The canal-like structure (underlying the ventral ridge) which joins the two pusules in *A*. *thermaeum* (see Figs 6, 8) has also been mentioned for other dinoflagellates by Kofoid and Swezy (1921), but further electron microscopy is necessary to elucidate this structure and whether it is associated with the flagellar system (as are the pusules, see Dodge 1972), or has other possible functions (see Klut *et al*. 1987). The elongate vesicles surrounding the pusules of *A*. *thermaeum* are similar to those described for *A*. *carterae* by Dodge and Crawford (1968), but appear quite different from those observed by Murray *et al*. (2004) for other *Amphidinium* species (smaller and more rounded).

The unusual striations or furrows very rarely observed on the hypocone of *A*. *thermaeum* may indicate some relation to *A*. *klebsii* (Kofoid and Swezy 1921, Lebour 1925), cells of which were described by Herdman (1924b) as having an orange or reddish spot in the epicone. Such an epiconal spot was never observed in *A*. *thermaeum*, which instead displayed 4–5 adjacent vacuolar bodies appearing as depressions inside the hypocone's left ventral side (see Figs 26, 27), a structure never reported before and possibly a species-specific feature. The rarely observed and unusual formation of one or two large vacuoles in the hypocone may be part of the life cycle or the result of cell stress. The dual or dividing central pyrenoids observed in some *A*. *thermaeum* cells, although not commonly reported in dinoflagellates (e.g., Dodge and Crawford 1971, Pearce and Hallegraeff 2004), have been previously seen in *A*. *massartii* (Biecheler 1952).

Cell division in hyaline cysts has also been reported for other representatives of the genus (see Table 2), but the amount of daughter cells was typically two or even three (similar to those of *A*. *steinii* Lemmermann, 1910), and never as many in number as those mentioned by Barlow and Triemer (1988) for *A*. *klebsii*. The species *A*. *thermaeum* is a swimming dinoflagellate in most of the life cycle with a short cyst stage and limited amount of daughter cells (i.e., 2–3).

Due to the lack of cultured material or lack of advanced taxonomical methods, it is uncertain how many of the previously reported *Amphidinium* species are ac-

tually independent taxa or synonymous, and whether critical morphological details have been overlooked or misreported. It is very likely that there are further species to be resolved in and assigned to the genus *Amphidinium sensu stricto*. For instance, since the *A. klebsii* strain JL9 (accession number AF260381) and the *A. massartii* strain CCMP1821 (accession number AY455670) genetically differentiate substantially (i.e., on an interspecific level) from the other two *A.* cf. *massartii* strains examined (AKLV01 and AKLSP01, see also Murray *et al*. 2004), morphological reexamination of several such phenotypes is necessary. Furthermore, the fact that the *A. mootonorum* strain MFJ18 and the *A. herdmanii* strains MFJ5 and MFJ10 differentiate very little genetically (i.e., their sequences diverge on an intraspecific rather than interspecific level compared to other *Amphidinium* species examined herein) could possibly indicate a recent speciation event, but cannot otherwise be explained without further investigating these strains. Additionally, *Amphidinium* specimens described (as '*A. operculatum*') by Calkins (1902) and Zimmermann (1930) need to be reinvestigated, including various other newly presented species (e.g., described in Conrad and Kufferath 1954, Schiller and Diskus 1955).

Acknowledgments. We appreciate the help of the following staff members of the University of Athens: A. Parmakelis and S. Amillis (DNA analyses and phylogeny), P. Apostolakos and C. Katsaros (use of fluorescent microscopy facilities), Sofia Papaioannou (latin amendment). We also thank the two anonymous reviewers for their comments on improving the manuscript. This work represents part of a doctoral thesis funded by the 'Irakleitos' Fellowships for Research of 'NKUA-Environment' and co-financed within the Op. Education by the European Social Fund and National Resources.

REFERENCES

Al-Qassab S., Lee W. J., Murray S., Simspon A. G. B., Patterson D. J. (2002) Flagellates from stromatolites and surrounding sediments in Shark Bay, western Australia. *Acta Protozool*. **41:** 91–144

Altschul S. F., Gish W., Miller W., Myers E. W., Lipman, D. J. (1990) Basic local alignment search tool. *J. Mol. Biol*. **215:** 403–410

Anissimowa N. W. (1926) Neue Peridineen aus den Salzgewässern von Staraja Russa (Gouv. Nowgorod). *Russk. Gidrobiol. Ž.* **5:** 188–193

Baig H. S., Saifullah S. M., Dar A. (2006) Occurrence and toxicity of *Amphidinium carterae* Hulburt in the North Arabian Sea. *Harmful Algae* **5:** 133–140

Barlow S., Triemer R. E. (1988) Alternate life history stages in *Amphidinium klebsii* (Dinophyceae, Pyrrophyta). *Phycologia* **27:** 413–420

Bergholtz T., Daugbjerg N., Moestrup Ø., Fernández-Tejedor M. (2005) On the identity of *Karlodinium veneficum* and description of *Karlodinium armiger* sp. nov. (Dinophyceae), based on light and electron microscopy, nuclear-encoded LSU rDNA, and pigment composition. *J. Phycol*. **42:** 170–193

Biecheler B. (1952) Recherches sur les Péridiniens. *Bull. Biol. France Belg*. **36 (Suppl.):** 1–149

Blanco A. V., Chapman G. B. (1987) Ultrastructural features of the marine dinoflagellate *Amphidinium klebsii* (Dinophyceae). *Trans. Am. Microsc. Soc.* **106:** 201–213

Botes L., Price B., Waldron M., Pitcher G. C. (2002) A simple and rapid scanning electron microscope preparative technique for delicate "Gymnodinioid" dinoflagellates. *Microsc. Res. Tech*. **59:** 128–130

Calado A. J., Moestrup Ø. (2005) On the freshwater dinoflagellates presently included in the genus *Amphidinium*, with a description of *Prosoaulax* gen. nov. *Phycologia* **44:** 112–119

Calkins G. N. (1902) Marine protozoa from Woods Hole. *Bull. U.S. Fish. Comm*. **21:** 413–468

Campbell P. H. (1973) Studies on brackish water phytoplankton. University of North Carolina. Sea Grant Publication UNC-SG--73-07. Sea Grant Program, Chapel Hill, NC

Claparède E., Lachmann J. (1859) Études sur les Infusoires et les Rhizopodes 2. *Mém. Inst. Natl. Genev*. **6:** 261–482

Conrad W., Kufferath H. (1954) Recherches sur les eaux Saumâtres des environs de Lilloo. II Partie Descriptive. Algues et Protistes – Considérations Écologiques. *Mém. Inst. R. Sci. Nat. Belg*. **127:** 1–346

Daugbjerg N., Hansen G., Larsen J., Moestrup Ø. (2000) Phylogeny of some of the major genera of dinoflagellates based on ultrastructure and partial LSU rDNA sequence data, including the erection of three new genera of unarmoured dinoflagellates. *Phycologia* **39:** 302–317

Dodge J. D. (1972) The ultrastructure of the dinoflagellate pusule: a unique osmo-regulatory organelle. *Protoplasma* **75:** 285–302

Dodge J. D., Crawford R. M. (1968) Fine structure of the dinoflagellate *Amphidinium carteri* Hurlburt. *Protistologica* **4:** 231–242

Dodge J. D., Crawford R. M. (1971) A fine-structural survey of dinoflagellate pyrenoids and food-reserves. *Bot. J. Linn. Soc*. **64:** 105–115

Farmer M. A., Roberts K. R. (1989) Comparative analysis of the dinoflagellate flagellar apparatus. III. Freeze substitution of *Amphidinium rhynchocephalum*. *J. Phycol*. **25:** 280–292

Felsenstein J. (1985) Confidence limits on phylogenies: an approach using the bootstrap. *Evolution* **39:** 783–791

Felsenstein J., Churchill G. A. (1996) A hidden Markov model approach to variation among sites in rate of evolution. *Mol. Biol. Evol*. **13:** 93–104

Fensome R. A., Taylor F. J. R., Norris G., Sarjeant W. A. S., Wharton D. I., Williams G. L. (1993) A classification of living and fossil dinoflagellates. American Museum of Natural History, Micropaleontology Special Publication 7. Sheridan Press, Hanover, PA

Flø Jørgensen M., Murray S., Daugbjerg N. (2004a) *Amphidinium* revisited. I. Redefinition of *Amphidinium* (Dinophyceae) based on cladistic and molecular phylogenetic analyses. *J. Phycol*. **40:** 351–365

Flø Jørgensen M., Murray S., Daugbjerg N. (2004b) A new genus of athecate interstitial dinoflagellates, *Togula* gen. nov., previously encompassed within *Amphidinium sensu* lato: Inferred from light and electron microscopy and phylogenetic analyses of partial large subunit ribosomal DNA sequences. *Phycol. Res*. **52:** 284–299

Fukuyo Y. (1981) Taxonomical study on benthic dinoflagellates collected in coral reefs. *Bull. Jpn. Soc. Sci. Fish.* **47:** 967–978

Gaines G., Elbrachter M. (1987) Heterotrophic nutrition. In: The Biology of Dinoflagellates, (Ed. F. J. R. Taylor). Blackwell Scientific Publicatıons, London, 224–268

Gómez F. (2007) Gymnodinioid dinoflagellates (Gymnodiniales, Dinophyceae) in the open Pacific Ocean. *Algae* **22:** 273–286

Grell K. G., Wohlfarth-Bottermann K. E. (1957) Licht- und elektronenmikroskopische Untersuchungen an dem Dinoflagellaten *Amphidinium elegans* n. sp. *Zeitschr. Zellforsch.* **47:** 7–17

Hansen G., Daugbjerg N. (2004) Ultrastructure of *Gyrodinium spirale*, the type species of *Gyrodinium* (Dinophyceae), including a phylogeny of *G. dominans*, *G. rubrum* and *G. spirale* deduced from partial LSU rDNA sequences. *Protist* **155:** 271–294

Herdman E. C. (1922) Notes on dinoflagellates and other organisms causing discolouration of the sand at Port Erin II. *Proc. Trans. Liverpool Biol. Soc.* **36:** 15–30

Herdman E. C. (1924a) Notes on dinoflagellates and other organisms causing discolouration of the sand at Port Erin III. *Proc. Trans. Liverpool Biol. Soc.* **38:** 58–63

Herdman E. C. (1924b) Notes on dinoflagellates and other organisms causing discolouration of the sand at Port Erin IV. *Proc. Trans. Liverpool Biol. Soc.* **38:** 75–84

Herdman W. A. (1911) On the occurrence of *Amphidinium operculatum* Clap. & Lach. in vast quantities at Port Erin (Isle of Man). *J. Linnean Soc. Zool.* **32:** 71–75

Huelsenbeck J. P., Ronquist F. (2001) MrBays: Bayesian inference of phylogenetic trees. *Bioinformatics* **17:** 754–755

Hulburt E. M. (1957) The taxonomy of unarmored Dinophyceae of shallow embayments on Cape Cod, Massachusetts. *Biol. Bull. Mar. Biol. Lab. Woods Hole* **112:** 196–219

Kimura M. (1980) A simple method for estimating evolutionary rates of base substitutions through comparative studies of nucleotide sequences. *J. Mol. Evol.* **16:** 111–120

Klut M. E., Bisalputra T., Antia N. J. (1987) Some observations on the structure and function of the dinoflagellate pusule. *Can. J. Bot.* **65:** 736–744

Klut M. E., Bisalputra T., Antia N. J. (1989) Some details of the cell surface of two marine dinoflagellates. *Bot. Mar.* **32:** 89–95

Kofoid C. A., Swezy O. (1921) The free-living unarmoured Dinoflagellata. *Mem. Univ. Calif.* **5:** 1–562

Koukaras K., Nikolaidis G. (2004) *Dinophysis* blooms in Greek coastal waters (Thermaikos Gulf, NW Aegean Sea). *J. Plankton Res.* **26:** 445–457

Larsen J. (1985) Algal studies of the Danish Wadden Sea. II. A taxonomic study of psammobious dinoflagellates. *Op. Bot.* **79:** 14–37

Larsen J., Patterson D. J. (1990) Some flagellates (Protista) from tropical marine sediments. *J. Nat. Hist.* **24:** 801–937

Lebour M. V. (1925) The dinoflagellates of northern seas. Mar. Biol. Ass. U.K., Plymouth, U.K.

Lee J. J., Olea R., Cevasco M., Pochon X., Correia M., Shpigel M., Pawlowski J. (2003) A marine dinoflagellate, *Amphidinium eilatiensis*, sp. nov., from the benthos of a mariculture sedimentation pond in Eilat, Israel. *J. Eukaryot. Microbiol.* **50:** 439–448

Lemmermann E. (1910) Algen I. (Schizophyceen, Flagellaten, Peridineen). Dritter Band. Kryptogamenflora der Mark Brandenburg und angrenzender Gebiete, Leipzig, Gebrüder Borntraeger

Lenaers G., Maroteaux L., Michot B., Herzog M. (1989) Dinoflagellates in evolution. A molecular phylogenetic analysis of large subunit ribosomal RNA. *J. Mol. Evol.* **29:** 29–40

Maranda L., Shimizu Y. (1996) *Amphidinium operculatum* var. nov. gibbosum (Dinophyceae), a free-swimming marine species producing cytotoxic metabolites. *J. Phycol.* **32:** 873–879

Massart J. (1920) Recherches sur les organismes inférieurs VIII. Sur la motilité des flagellates. *Bull. Acad. R. Belg. Cl. Sci.* **VI:** 116–141

Mohammad-Noor N., Daugbjerg N., Moestrup Ø., Anton A. (2006) Marine epibenthic dinoflagellates from Malaysia – a study of live cultures and preserved samples based on light and scanning electron microscopy. *Nord. J. Bot.* **24:** 629–690

Moncheva S., Gotsis-Skretas O., Pagou K., Krastev A. (2001) Phytoplankton blooms in Black Sea and Mediterranean coastal ecosystems subjected to anthropogenic eutrophication: similarities and differences. *Estuar. Coast. Shelf Sci.* **53:** 281–295

Murray S., Patterson D. J. (2002) The benthic dinoflagellate genus *Amphidinium* in south-eastern Australian waters, including three new species. *Eur. J. Phycol.* **37:** 279–298

Murray S., Flø Jørgensen M., Daugbjerg N., Rhodes L. (2004) *Amphidinium* revisited II: Resolving species boundaries in the *Amphidinium operculatum* species complex (Dinophyceae) including the descriptions of *Amphidinium trulla* sp. nov. and *Amphidinium gibbosum* comb. nov. *J. Phycol.* **40:** 366–382

Nikolaides G., Moustaka-Gouni M. (1990) The structure and dynamics of phytoplankton assemblages from the inner part of the Thermaikos Gulf, Greece. I. Phytoplankton composition and biomass from May 1988 to April 1989. *Helgol. Mar. Res.* **44:** 487–501

Page R. D. M. (1996) TREEVIEW: An application to display phylogenetic trees on personal computers. *Comp. Appl. Biosc.* **12:** 357–358

Pearce I., Hallegraeff G. M. (2004) Genetic affinities, ecophysiology and toxicity of *Prorocentrum playfairii* and *P. foveolata* (Dinophyceae) from Tasmanian freshwaters. *Phycologia* **43:** 271–281

Popovský J., Pfiester L. A. (1990) Dinophyceae (Dinoflagellida). In: Süßwasserflora von Mitteleuropa, Band 6, (Eds. H. Ettl, J. Gerloff, H. Heynig, D. Mollenhaver). Gustav Fischer Verlag, Jena, 1–272

Posada D., Crandall K. A. (1998) Modeltest: testing the model of DNA substitution. *Bioinformatics* **14:** 817–818

Saiki R. K., Gelfand D. H., Stoffel S., Scharf S. J., Higuchi R., Horn G. T., Mullis K. B., Erlich H. A. (1988) Primer-directed enzymatic amplification of DNA with a thermostable DNA polymerase. *Science* **239:** 487–491

Schiller J. (1933) Dinoflagellatae (Peridineae). Monographischer Behandlung. 1. Teil. In: Dr. L. Rabenhorst's Kryptogamen-Flora von Deutschland, Österreich und der Schweiz, Zehnter Band, Flagellatae, Dritte Abteilung, (Ed. R. Kolkwitz). Akademische Verlagsgesellschaft M.B.H. Leipzig (1971 Reprint: Johnson, New York), 1–617

Schiller J., Diskus A. (1955) Über ein neues *Amphidinium* von einer Laguneninsel bei Venedig. *Anz. Österreichische Akad. Wissensch. (Math. Natures. Klasse)* **9:** 100–103

Scholin C. A., Herzog M., Sogin M., Anderson D. M. (1994) Identification of group and strain-specific genetic markers for globally distributed *Alexandrium* (Dinophyceae). II. Sequence analysis of a fragment of the LSU rRNA gene. *J. Phycol.* **30:** 999–1011

Sparmann S. F., Leander B. S., Hoppenrath M. (2008) Comparative morphology and molecular phylogeny of *Apicoporus* n. gen.: A new genus of marine benthic dinoflagellates formerly classified within *Amphidinium*. *Protist* **159:** 383–399

Stamatakis A. (2006) RAxML-VI-HPC: Maximum likelihood--based phylogenetic analyses with thousands of taxa and mixed models. *Bioinformatics* **22:** 2688–2690

Stamatakis A., Hoover P., Rougemont J. (2008) A rapid bootstrap algorithm for the RAxML web-servers. *Syst*. *Biol*. **75:** 758–771

Steidinger K. A. (1983) A re-evaluation of toxic dinoflagellate biology and ecology. In: Progress in Phycological Research, Vol. 2, (Eds. F. E. Round, D. Chapman). Elsevier, North Holland, Amsterdam, 147–188

Steidinger K. A., Tangen K. (1997) Dinoflagellates. In: Identifying Marine Phytoplankton, (Ed. C. R. Tomas). Academic Press, San Diego, 387–589

Swofford D. L. (2000) PAUP (Version 4, Beta 10). Phylogenetic Analysis Using Parsimony. Sinauer Associates, Sunderland, MA

Tamura K., Dudley J., Nei M., Kumar S. (2007) MEGA4: Molecular Evolutionary Genetics Analysis (MEGA) software version 4.0. *Mol*. *Biol*. *Evol*. **24:** 1596–1599

Taylor D. L. (1971) Taxonomy of some common *Amphidinium* species. *Br*. *Phycol*. *J*. **6:** 129–133

Thompson J. D., Gibson T. J., Plewniak F., Jeanmougin F., Higgins D. G. (1997) The ClustalX windows interface: flexible strategies for multiple sequence alignment aided by quality analysis tools. *Nucleic Acids Res*. **25:** 4876–4882

Yasumoto T., Seino N., Murakami Y., Murata M. (1987) Toxins produced by benthic dinoflagellates. *Biol*. *Bull*. **172:** 128–131

Zhang H., Bhattacharya D., Lin S. (2007) A three-gene dinoflagellate phylogeny suggests monophyly of Prorocentrales and a basal position for *Amphidinium* and *Heterocapsa*. *J*. *Mol*. *Evol*. **65:** 463–474

Zhang Z., Schwartz S., Wagner L., Miller W. (2000) A greedy algorithm for aligning DNA sequences. *J*. *Comput*. *Biol*. **7:** 203–214

Zimmermann W. (1930) Neue und wenig bekannte Kleinalgen von Neapel. I–IV. *Zeitschr*. *Bot*. **23:** 419–442

Received on 25th February, 2009; revised version on 20th May, 2009; accepted on 22nd May, 2009